



ELSEVIER

Physica A 220 (1995) 192–216

PHYSICA A

# Lipid chain packing and lipid–protein interaction in membranes<sup>\*</sup>

Deborah R. Fattal, Avinoam Ben-Shaul

*Department of Physical Chemistry and the Fritz Haber Research Center, The Hebrew University of Jerusalem, Jerusalem 91904, Israel*

---

## Abstract

This article describes briefly several applications of a molecular theory of lipid organization in membranes to systems of biophysical interest. After introducing the basic concepts of this mean field theory we outline three of its recent applications. i) Calculations of lipid chain conformational statistics in membrane bilayers, and comparison of the results (e.g. bond orientational order parameters) to experiment and molecular dynamics simulations. Good agreement is found. ii) A molecular model for lipid–protein interactions, which explicitly considers the effects of a rigid hydrophobic protein on the elastic (conformational) properties of the lipid bilayer. We also analyze the role of the ‘hydrophobic mismatch’ between the protein and lipid bilayer thickness. iii) A molecular level calculation of the vesicle to micelle transition, attendant upon the addition of (‘curvature loving’) surfactant to a lipid bilayer vesicle. Future applications, e.g. to the calculation of the free energy barriers involved in membrane fusion are briefly mentioned.

---

## 1. Introduction

In this lecture we outline a mean field theory of lipids in membrane bilayers and demonstrate some of its recent biophysical applications [1,2]. The central quantity in this theory is the singlet probability of lipid tail conformations, which we derive by minimizing the system free energy subject to packing constraints on the lipid conformational statistics. These packing constraints can be expressed in a simple mathematical

---

<sup>\*</sup> A summary of a lecture given at the XXIV winter meeting of the Mexican Statistical Physics Society, Cuernavaca, Mexico, January 1995. This article is printed with the permission of CRC Press. The contents of this lecture largely overlap: Nonmedical Applications of Liposomes, Y. Barenholtz and D.D. Lasic, Eds., Vol. 1, Liposomes: Theory and Basic Science (CRC Press, Boca Raton, FL) Ch. 5, in press.

form, based on the assumption that the hydrophobic core of the membrane (in its fluid state) is uniformly packed by chain segments [3–5]. The packing constraints depend on the aggregation geometry; that is, on the curvature of the hydrocarbon–water interface and on the average area per head group, as measured at this interface. Using the singlet distribution one can calculate any desired conformational property and, in the mean field approximation, any thermodynamic property of interest [1,2,6–8].

The mean field approach described here is obviously approximate as far as thermodynamic properties are concerned. But, as will be demonstrated in Section 3, its predictions with regard to ‘single chain’ conformational properties show good agreement with both experiment and large scale computer simulations. As a molecular level theory it is certainly more detailed than phenomenological, e.g. continuum theories of the lipid membrane, or models based on geometric packing considerations [3–5]. On the other hand, it is less detailed (yet much simpler to implement) than many-molecule computer simulations, such as molecular dynamics (MD) or Monte Carlo (MC) calculations. (For computer simulations of lipid membranes see e.g. [9–13]).

Generally, in mean field theories of the lipid membrane, one treats in detail the conformational properties of one, ‘central’ molecule, but the effects of neighboring molecules are treated approximately. They are assumed to provide a ‘mean field’ for the ‘motion’ of the central molecule. In general, the mean field appears as a variational parameter (or parameters) in the singlet probability distribution of the central chain and its numerical evaluation involves a solution of ‘self-consistency’ equations. For instance, in the theory presented in the next section, the mean field acting on the central lipid molecule is represented by the ‘lateral pressure profile’ exerted on this chain by its neighbors. (As the average area per molecule decreases, the lateral pressure increases, and the lipid chains are farther stretched along the membrane normal). The self-consistency equations represent the packing constraints on the lipid chains which, as mentioned above, reflect the assumption of a uniform, liquid-like, hydrophobic core. Some applications of the theory presented here are described in [21–27]. For other mean field theories see e.g. [14–20,28–30].

## 2. The singlet distribution of chain conformations

A bilayer membrane can be treated as a two-dimensional (2D) film, composed of a central hydrophobic region comprising the hydrocarbon chains (‘tails’) of the lipids and two interfacial regions containing their polar head groups; Fig. 1. We shall focus on the conformational properties of the lipid chains. The interactions involving the polar heads will only be treated in an approximate, ‘phenomenological’ fashion. The main reason for that is the highly specific nature of these interactions which depend sensitively on the size, charge (e.g. ionic vs. zwitterionic) and chemical composition of the head groups.

The membrane free energy can be expressed as a sum of three terms,

$$F = F_t + F_s + F_h = 2N(f_t + f_s + f_h), \quad (1)$$

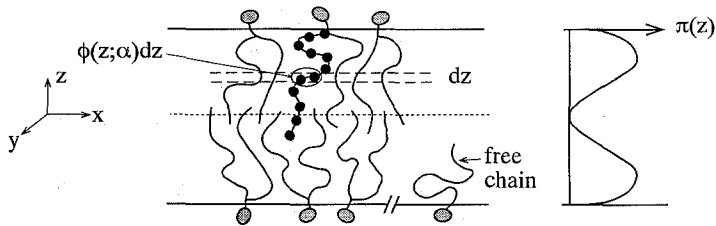


Fig. 1. Schematic illustration of a (planar) lipid bilayer and the quantities appearing in the derivation of the singlet probability of chain conformations, see (5):  $\phi(z; \alpha)dz$  denotes the number of chain segments, which, for a chain in conformation  $\alpha$ , fall within the shell  $z, z + dz$ . The 'free chain' is a (hypothetical) chain with no neighbors around it. The lateral pressure profile  $\pi(z)$  schematically illustrated in the figure, accounts for the pressure exerted on a given (stretched) chain by its neighbors in the bilayer.

representing, respectively, the contributions of the hydrocarbon tails, the surface free energy corresponding to the hydrocarbon–water interface and the (solution mediated) interaction free energy between the head groups. The  $f_i$ 's ( $i = t, s, h$ ) are the corresponding free energies, per molecule, with  $2N$  denoting the number of molecules in the membrane ( $N$  per monolayer, on the average). All three terms depend on the lipid composition of the two monolayers comprising the membrane bilayer and the ambient solution conditions, as well as on the membrane area and curvature. The interplay between these terms dictates the equilibrium geometry of the membrane (area and curvature), fluctuations around the equilibrium state and all microscopic (e.g. chain conformations) and thermodynamic (e.g. elastic) properties of the membrane. We shall first consider each term separately, devoting most of the discussion to  $F_t$ .

### 2.1. Tail free energy

The formalism outlined below can be applied to a bilayer membrane of arbitrary lipid composition, whether symmetric or nonsymmetric with respect to the two monolayers, as well as to an arbitrary membrane thickness and/or curvature. The theory can be applied to other amphiphilic aggregates such as micelles (see also Section 5), as well as to systems containing hydrophobic inclusions (see Section 4). However, to introduce the basic concepts involved, let us consider the simplest possible membrane, namely, a planar symmetric bilayer composed of a single lipid component. Furthermore, let us assume that the lipids are single (saturated) chain amphiphiles, of the form  $\mathcal{P}-(\text{CH}_2)_{n-1}-\text{CH}_3$ , with  $\mathcal{P}$  denoting the polar head group. The generalization to doubly tailed lipids, including nonsaturated chains is straightforward, as described in Section 3.

We now turn to derive an expression for  $P(\alpha)$ , the probability of finding the lipid hydrocarbon chain in conformation  $\alpha$ . A common and quite accurate specification of  $\alpha$  can be using the rotational isomeric state (RIS) model of acyl chains [31], i.e., by the trans/gauche sequence of the  $\text{CH}_2-\text{CH}_2$  bonds along the chain, and by the overall orientation of the chain (specified by three Euler angles) relative to some arbitrary fixed system of coordinates (see Fig. 1).

Using  $P(\alpha)$  we can calculate any desirable ‘single chain’ conformational property. Of particular interest are those properties which can be measured experimentally, or calculated by detailed computer simulations. In addition to the physical significance of these properties, their calculation provides a test for the expression which we shall derive for  $P(\alpha)$ . The most commonly measured or calculated conformational properties are the bond orientational order parameters and the segment spatial distributions to be defined later on. Furthermore,  $P(\alpha)$  can be used to calculate various thermodynamic properties of interest, such as the free energy per chain,  $f_t$ , and related quantities such as the curvature elasticity moduli of the membrane [6,32–35].

The free energy per chain is given, in terms of  $P(\alpha)$ , as

$$f_t = \sum_{\alpha} P(\alpha) \epsilon(\alpha) + kT \sum_{\alpha} P(\alpha) \ln P(\alpha), \quad (2)$$

where  $k$  is Boltzmann’s constant,  $T$  is the temperature and  $\epsilon(\alpha)$  is the internal (trans/gauche) energy of a chain in conformation  $\alpha$ . More specifically,  $\epsilon(\alpha) = n_g(\alpha)e_g + n_t(\alpha)e_t$  where  $n_g(\alpha)$  and  $n_t(\alpha)$  are the numbers of gauche and trans conformers along the chain, with  $e_g$  and  $e_t$  representing their respective energies. One usually sets  $e_t = 0$  implying  $e_g \simeq 500$  cal/mole. The first term in (2) is the energetic contribution to the chain free energy, while the second is the conformational entropy contribution. Both depend on the curvature of the membrane, its thickness and its chemical composition.

We derive the desired (equilibrium) singlet probability distribution (spd) by minimization of the free energy functional  $f_t$  with respect to  $\{P(\alpha)\}$ , subject to whichever constraints  $P(\alpha)$  must fulfill. Except for the trivial normalization condition ( $\sum_{\alpha} P(\alpha) = 1$ ) the only additional constraint on  $P(\alpha)$  results from the assumption that the liquid-like hydrophobic core is uniformly packed by chain segments. The mathematical expression of this constraint is

$$\int ds \sigma(s) \sum_{\alpha} P(\alpha; s) \psi(\mathbf{r}; \alpha, s) = \rho(\mathbf{r}) \quad (\text{all } \mathbf{r}), \quad (3)$$

which, for a symmetric planar bilayer, reduces to

$$\sum_{\alpha} P(\alpha) [\phi(z; \alpha) + \phi(-z; \alpha)] = a\rho \quad (\text{all } z). \quad (4)$$

The quantities appearing in (3) and (4) are as follows:  $P(\alpha; s)$  denotes the spd corresponding to chains originating from point  $s$  of the hydrocarbon–water interface; for simplicity  $s$  may be regarded as the head group position.  $\sigma(s)$  is the lateral density of head groups at the interface; i.e.  $\sigma(s)ds$  is the number of chains originating from an area element  $ds$  at the interface. It should be noted that the  $s$  integration in (3) includes both interfaces. The quantity  $\psi(\mathbf{r}; \alpha, s)d\mathbf{r}$  denotes the number of segments of a chain in conformation  $\alpha$ , originating at  $s$ , which fall within a small volume element  $d\mathbf{r}$  (around  $\mathbf{r}$ ) of the hydrophobic core.  $\rho(\mathbf{r})$  is the average segment density at  $\mathbf{r}$  which, for a ‘compact’ core, is constant:  $\rho(\mathbf{r}) = \rho = 1/\nu$  where  $\nu$  is the average volume per chain segment in the hydrophobic core.

In passing from (3) to (4) we have specifically considered a symmetric planar, single component, bilayer. For this system we have  $\sigma(s) = \text{constant} = 1/a$  where  $a$  is the average cross sectional area per chain, measured at the hydrocarbon–water interface. This important structural characteristic of the membrane is usually referred to as ‘the area per head group’. Also, for the simple bilayer,  $P(\alpha; s) = P(\alpha)$  is independent of  $s$ . We now choose a coordinate system whose origin is at the bilayer midplane, with its  $z$ -axis pointing towards the ‘upper’ interface. Clearly, for a chain with head group coordinates  $s = (x, y) = (0, 0)$  the quantity  $\psi(r; \alpha, s) = \psi(r; \alpha, 0)$  is only a function of  $z$ . Then the left hand side of (3) can be integrated over  $x$  and  $y$  to obtain (4), in which  $\phi(z; \alpha) dz = (\int \psi(r; \alpha) dx dy) dz$  is simply the number of segments of an  $\alpha$ -chain falling within the shell  $z, z + dz$  of the hydrophobic core; see Fig. 1. The two terms within the square brackets in (4) represent the contribution to the segment density in  $z$ , due to chains anchored to the ‘upper’ and ‘lower’ interfaces, respectively. Of course, (4) could be immediately written down for the symmetric bilayer. We have emphasized here that it is a special case of the more general form (3), which will be of use in Section 4.

We now minimize (2) subject to (4) and obtain

$$P(\alpha) = \frac{1}{q} \exp \left[ -\beta \epsilon(\alpha) - \beta \int \pi(z) \phi(z; \alpha) dz \right], \quad (5)$$

with

$$q = \sum_{\alpha} \exp \left[ -\beta \epsilon(\alpha) - \beta \int \pi(z) \phi(z; \alpha) dz \right] \quad (6)$$

representing the conformational partition function of the chain, and  $\beta \equiv 1/kT$ . The quantities  $\{\pi(z)\}$  in these equations are the Lagrange multipliers conjugate to the packing constraints (4). They have the dimensions and the physical significance of ‘lateral pressures’, as discussed in detail elsewhere [1,2,21]; see Fig. 1. The numerical values of the  $\{\pi(z)\}$  are determined by the self-consistency equations resulting from substitution of (5) into the packing constraint (4). This results in a set of nonlinear algebraic equations which can be solved, quite simply and efficiently for any chain model.

Substituting (5) into (2) we obtain

$$f_t = -kT \ln q - a\rho \int \pi(z) dz. \quad (7)$$

Thus, after evaluating the  $\pi(z)$  we can calculate any chain conformational property derivable from  $P(\alpha)$  through (5), or any thermodynamic property derivable from  $f_t$ , using (7). Clearly, all the results depend sensitively, through  $\pi(z)$ , on the value of the area per head group,  $a$ .

The results (5)–(7), corresponding to the symmetric, planar, single component bilayer, can be easily generalized to more complex systems. Let us briefly mention a few cases of interest.

(i) *Curved bilayers.* Here  $a$  is not constant, but, rather  $a = a(c_1, c_2, z)$ , where  $c_1$  and  $c_2$  denote the local interfacial curvatures. ( $c_i = 1/R_i$  are the principal curvatures;  $R_i$  denoting the radius of curvature). The packing constraints (4) should be replaced by

$$\begin{aligned} \chi_E \sum_{\alpha} P_E(\alpha) \phi(z; \alpha) + \chi_I \sum_{\beta} P_I(\beta) \phi(z; \beta) &= \rho a(z) \\ &= a(0) [1 + (c_1 + c_2)z + c_1 c_2 z^2], \end{aligned} \quad (8)$$

with  $P_E(\alpha)$  and  $P_I(\beta)$  representing the spd's of chains originating at the 'external' ( $E$ ) and 'internal' ( $I$ ) monolayers composing the bilayer; e.g. of a vesicle. (Clearly for a spherical vesicle of radius  $R$ ,  $c_1 = c_2 = 1/R$ ). The quantities  $\chi_E$  and  $\chi_I$  are the 'mole fractions' of lipids in the two monolayers;  $\chi_E = N_E/N$  and  $\chi_I = N_I/N$  ( $\chi_E + \chi_I = 1$ ,  $N_E + N_I = N$ ) with  $N_E$  and  $N_I$  denoting the number of chains originating from the  $E$  and  $I$  interfaces, respectively.

The free energy per molecule is now given by

$$\begin{aligned} f_i &= \chi_E \sum_{\alpha} P_E(\alpha) [\epsilon(\alpha) + kT \ln P_E(\alpha)] \\ &+ \chi_I \sum_{\beta} P_I(\beta) [\epsilon(\beta) + kT \ln P_I(\beta)]. \end{aligned} \quad (9)$$

Minimization of (9) with respect to (8) yields for  $P_E(\alpha) = P_E(\alpha; a, c_1, c_2)$  and  $P_I(\beta) = P_I(\beta; a, c_1, c_2)$  expressions similar to (5), except that now  $\pi(z)$  and  $q_E(q_I)$  depend not only on  $a$  but also on  $c_1$  and  $c_2$ .

(ii) *Micelles.* To model micelles is to account for the curvature dependence of  $a(z)$ . For a cylindrical micelle for instance, as will be discussed in Section 5, instead of (4) we have

$$\sum_{\alpha} P(\alpha) \phi(r; \alpha) = \rho a(R) r/R, \quad (10)$$

where  $R$  is the radius of the micelle and  $r$  is the radial distance from the cylinder axis. Here again  $P(\alpha)$  is of the form (5), but now the pressure profile  $\{\pi(r)\}$  depends on the micellar radius  $R$ . For micelles composed of chains of a given length  $n$ , the average area per chain, at the interface,  $a(R)$ , is uniquely determined by  $R$  through the geometric packing condition  $a(R) = 2\nu/R$  where  $\nu$  is the chain volume. For simple alkyl chains,  $-(\text{CH}_2)_{n-1}-\text{CH}_3$ ,  $\nu \cong (n+1)\nu$  where  $\nu \simeq 27 \text{ \AA}^3$  is the specific volume of a  $\text{CH}_2$  group.

(iii) *Mixed systems.* Consider for instance a planar symmetric bilayer composed of two types of lipid chains,  $A$  and  $B$ . Then, instead of (4) we write

$$X_A \sum_{\alpha} P_A(\alpha) [\phi_A(z, \alpha) + \phi_A(-z; \alpha)]$$

$$+X_B \sum_{\beta} P_B(\beta) [\phi_B(z, \beta) + \phi_B(-z, \beta)] = a\rho, \quad (11)$$

where  $X_A$  and  $X_B = 1 - X_A$  are the mole fractions of the two types of chains. The free energy of this system is given by

$$F_t = N[X_A f_{t,A} + X_B f_{t,B}], \quad (12)$$

with  $f_{t,A}$  and  $f_{t,B}$  defined according to (2). Again, minimization of (12) subject to (11) yields  $P_A(\alpha)$  and  $P_B(\beta)$  of the form (5). The same  $\pi(z)$  appears in both expressions.

(iv) *Non-uniform membranes.* The presence of a hydrophobic solute in the membrane, say, an integral protein, ‘breaks’ the translational symmetry of the planar bilayer. Thus,  $P(\alpha; s)$  will depend on the head group position  $s$ , as measured for instance with respect to the position of the protein. In this more general case, we have

$$F_t = \int ds \sigma(s) f_t(s), \quad (13)$$

where  $f_t(s)$  is the local free energy of a chain originating at  $s$ . The relevant packing constraint is now (3). Minimization of (13) with respect to (3) yields [7]

$$P(\alpha; s) = \frac{1}{q(s)} \exp \left[ -\beta \epsilon(\alpha) - \beta \int d\mathbf{r} \lambda(\mathbf{r}) \psi(\mathbf{r}; \alpha, s) \right], \quad (14)$$

with the  $\lambda(\mathbf{r})$  corresponding to the Lagrange parameters conjugate to the packing constraints (3). In this case, due to the lower symmetry of the system, the calculations are considerably more involved (chains must be generated and classified for different points  $s$ ), but are feasible, as illustrated in Section 4 for a model of lipid protein interaction [7].

## 2.2. Head group and surface free energies

The chain free energy  $f_t$ , as given by (2) and (7), decreases as the average cross-sectional area per chain,  $a$ , increases. This follows simply from the fact that as  $a$  increases the lateral dimensions of the chains also increase, allowing for more conformational freedom. More precisely, the energetic contribution to the free energy  $\langle \epsilon_t \rangle = \sum P(\alpha) \epsilon(\alpha)$  increases with  $a$  since the average number of gauche bonds increases. However, the increase in conformational entropy (chain flexibility) overcompensates the increase in  $\langle \epsilon_t \rangle$ , resulting in a net decrease of  $f_t$ . Thus, the conformational free energy corresponds effectively to a repulsive interaction between chains. This implies a positive lateral pressure

$$\Pi_t = -\frac{\partial f_t}{\partial a} = -\rho \int \pi(z) dz > 0, \quad (15)$$

which tends to expand the bilayer.

The interaction between the head groups, whether electrostatic or steric, is generally also repulsive [1–3], i.e.

$$\Pi_h = -\frac{\partial f_h}{\partial a} > 0, \quad (16)$$

where  $f_h = F_h/2N$  is the average interaction free energy per head group.

The interfacial free energy  $F_s$  provides the opposing force to both inter-head group and inter-chain repulsions. The origin of this force is the ‘hydrophobic interaction’, resulting from the increased hydrocarbon–water contact area upon increasing  $a$ .  $f_s = F_s/2N$  is usually expressed as a simple surface energy,  $f_s = \gamma a$ , with  $\gamma$  (often taken as  $\gamma = 50$  dyn/cm =  $0.12$  kT/Å<sup>2</sup> at  $T = 300$  K) denoting the effective surface tension [3]. With this representation of  $f_s$  one has

$$\Pi_s = -\frac{\partial f_s}{\partial a} = -\gamma < 0. \quad (17)$$

The equilibrium area per head group,  $a_{eq}$ , is determined by the balance of the three forces, that is,

$$\Pi_t + \Pi_h + \Pi_s = 0. \quad (18)$$

Fig. 2 shows the three contributions,  $f_t$ ,  $f_s$  and  $f_h$  to the average free energy per molecule

$$f = f_t + f_s + f_h \quad (19)$$

as a function of the area per molecule in a planar bilayer. The chain contribution  $f_t(a)$  was calculated using (7) for three values of the chain length ( $n = 12, 14, 16$ ). The hydrocarbon tails correspond to simple alkyl chains,  $-(\text{CH}_2)_{n-1}-\text{CH}_3$ , and are modeled using the rotational isomeric state model. For  $f_s$  we have used  $f_s = \gamma a$  with  $\gamma = 0.12$  kT/Å<sup>2</sup>. The head group contribution is represented here by the simple (and common) form [3,7,5]

$$f_h = C/a, \quad (20)$$

where  $C$  is a phenomenological constant. For the calculations shown in Fig. 2 we have chosen  $C$  to yield  $a_{eq} = 32$  Å<sup>2</sup> for the  $n = 14$  chains ( $C = 48$  kT).

It should be stressed that (20) is a highly approximate representation of  $f_h$ . For more detailed models of  $f_h$  corresponding to electrostatic and/or steric repulsions see e.g. [27,36–43].

The free energy change  $\delta f(a) = f(a) - f(a_{eq})$  defines the area compressibility modulus  $\kappa_a$  according to [32]

$$\frac{1}{a_{eq}} \delta f(a) = \frac{1}{2} \kappa_a \left( \frac{\delta a}{a_{eq}} \right)^2. \quad (21)$$

From the data in Fig. 2 it follows that  $\kappa_a \sim 0.2$  kT/Å<sup>2</sup>. One can also calculate  $\delta f(a, c_1, c_2) = f(a, c_1, c_2) - f(a_{eq}, c_1^{eq}, c_2^{eq})$  and thus derive explicit expressions and

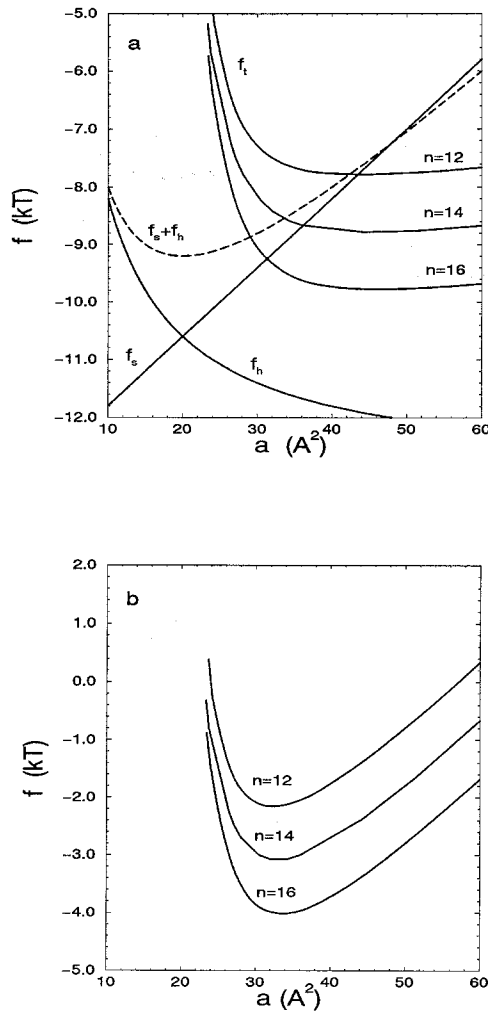


Fig. 2. (a) The variation of the chain ( $f_i$ ), head group ( $f_h$ ) and surface ( $f_s$ ) contributions to the average free energy per molecule, as a function of the average cross-sectional area per chain (head group),  $a$ ; see Eq. (19).  $f_h$  is calculated using (20) with  $C = 48$  kT.  $f_s = \gamma a$  with  $\gamma = 0.12$  kT/ $\text{\AA}^2$ .  $f_i$  is calculated using the meanfield theory for  $C_{12}$ ,  $C_{14}$  and  $C_{16}$  chains. (b) The sum of the three contributions above revealing that  $a_{eq}$  ( $\sim 32$   $\text{\AA}^2$ ) increases slowly with chain length.

numerical values for curvature elasticity moduli. The relevant formalism and its applications have been described in detail elsewhere [2,6]. The calculation of membrane elastic moduli is a particular *thermodynamic* application of the theory outlined in this section. Other thermodynamic applications are described in Sections 4 and 5.

### 3. Conformational properties

A common characteristic of conformational chain statistics in membranes is the orientational order profile of the C–H bonds along the lipid hydrocarbon tails [5,44–48]. The orientational order parameters are usually measured by nuclear magnetic resonance (NMR) methods, using selective (or nonselective) deuteration of the chains. Specifically, the measured quantity is the orientational order parameter of the C<sub>k</sub>–H (C<sub>k</sub>–D) bond (for  $-(\text{CH}_2)_{n-1}-\text{CH}_3$  chains,  $k = 1, \dots, n$ ) defined as

$$S_k = \langle P_2(\cos \theta_k) \rangle = \sum_{\alpha} P(\alpha) [3 \cos^2 \theta_k(\alpha) - 1] / 2, \quad (22)$$

where  $P_2(x) = (3x^2 - 1)/2$  is the second Legendre polynomial;  $\theta_k(\alpha)$  denoting, for a chain conformation  $\alpha$ , the angle between the  $k$ th bond and the membrane normal (the ‘director’). The C–H order parameters can be related to the skeletal order parameters,  $\tilde{S}_k$ , corresponding to the vectors  $\mathbf{r}_{k-1,k+1}$  connecting carbons  $k - 1$  and  $k + 1$  of the chain:  $\tilde{S}_k = -2S_k$  for all  $k$  except for the terminal methyl group ( $-\text{CH}_3$ ) for which  $\tilde{S}_n = -3S_n$  [48].

The orientational order parameter profiles provide a measure of chain flexibility, reflecting the ‘fluidity’ of the hydrophobic core. In the perfectly ordered state of the membrane, when all lipid chains are in their all-trans conformation, with the chain axis along the membrane normal, one has  $S_k = -0.5$  ( $\theta_k = \pi/2$ ) or  $\tilde{S}_k = 1$ , for all  $k = 1, \dots, n - 1$ . In the opposite limit, where bond orientations are random  $S_k = \tilde{S}_k = 0$ .

Bond order parameter profiles of (saturated) lipid chains in planar bilayers are typically characterized by a roughly constant value of  $S_k$  for, about, the first half of the chain (the ‘plateau region’), followed by a monotonic decrease of  $S_k$  towards the chain terminus. The last chain segments, those which reach and possibly cross (‘interdigitate’ through) the bilayer midplane are characterized by  $S_k \sim 0$ , indicating nearly random bond orientations. This behavior also indicates ‘high fluidity’ in the central part of the hydrophobic core, as compared to the regions bordering the interface where chain orientational ordering is relatively large. The magnitude of  $S_k$  in the plateau region increases as the membrane thickness  $d$  increases or, equivalently, as the average cross-sectional area per chain,  $a$ , decreases. This behavior is to be expected, since as  $d$  increases, the hydrocarbon chains must be further stretched out, resulting in a higher degree of chain ordering along the membrane normal. Note that this trend is a direct consequence of the tight (fluid-like) packing condition of the chains within the hydrophobic core. In other words, the packing constraints rather than, say, the relative trans/gauche energy of the chains are the important determinant of chain ordering in membranes. These qualitative trends have been quantitatively analyzed and confirmed by molecular level calculations based on Eq. (5) [24].

Bond orientational order parameters calculations using (5) for  $P(\alpha)$  have been presented for various systems. In Fig. 3 we show two sets of bond order parameter profiles, corresponding to the two hydrocarbon chains of palmitoyl-oleoyl-phosphatidylcholine (POPC) [26]. Here, the palmitoyl chain is a saturated  $-(\text{CH}_2)_{14}-\text{CH}_3$  alkyl chain

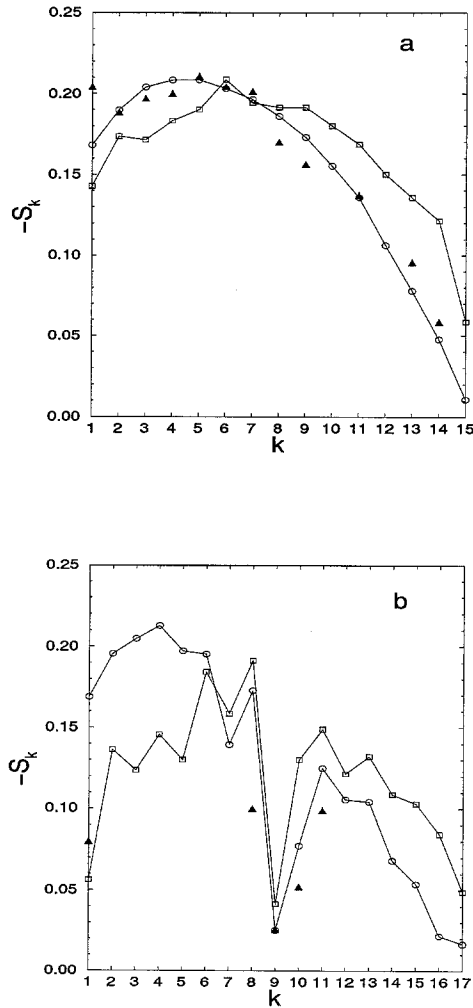


Fig. 3. Orientational order parameter profiles of the C–H bonds along the palmitoyl (a) and oleoyl (b) chains of DMPC (adapted from [26]).  $\blacktriangle$ : experimental results [44],  $\square$ : molecular dynamics calculations [9],  $\circ$ : mean field theory [26].

whereas the  $C_{17}$  (seventeen carbon) oleoyl chain contains one *cis* double bond, between carbons 8 and 9;  $-(CH_2)_7-(CH=CH)-(CH_2)_7-CH_3$ . The two chains are connected through the glycerol backbone which is further connected to the zwitterionic phosphatidylcholine head group. The results shown in Fig. 3 correspond to POPC molecules packed in a bilayer of (hydrophobic core) thickness  $d = 30.0 \text{ \AA}$ , at  $T = 300 \text{ K}$ . Simple packing considerations (see below) imply that this thickness corresponds to an average cross-sectional area per head group of  $a = 60.5 \text{ \AA}^2$ , which is also the average cross-sectional area of the lipid tail (composed of one oleoyl and one palmitoyl chain).

The POPC bilayer has been chosen primarily in order to compare the predictions of the mean field theory, Eq. (5), with those of a most comprehensive molecular dynamics (MD) simulation of the same system [9]. The MD results as well as (partial) experimental results for the POPC bilayer [44] are also shown in Fig. 3. The agreement between these sets of results is quite satisfactory considering the complexity of the system modeled. The typical 'plateau' region of the saturated chain is reproduced as well as the very distinctive drop in the orientational order parameter at the double bond region of the oleoyl chain. Differences in the  $S_k$  values appear mainly for the first few C–H bonds of the oleoyl chain. This, probably, is due to the approximate treatment of the glycerol backbone of the lipid from which the two chains emanate.

Despite the inherent approximations involved in the mean field analysis its predictions compare well with those derived from MD simulations. The difference in computation time between the two approaches is enormous. Obviously, MD simulations provide much more detailed information, including information on dynamical properties, which the mean field equilibrium theory cannot treat at all. Yet, even with the best interaction potentials known and the fastest computers available, the number of systems which can be studied in detail by MD methods to date is limited, and even those are followed over relatively short periods of time. On the other hand, the mean field approach described above, though approximate, can be easily applied to a very wide range of systems (e.g. different lipid compositions) and a wide range of conditions (e.g. membranes of different curvatures). Thus, as noted already in Section 1, while the quality of large scale computer simulations is rapidly growing, there are many systems and properties (e.g. curvature elastic moduli) which can only be studied by approximate, mean field, theories.

Another measurable structural characteristic of lipid membranes is the distribution of different chain segments across the bilayer hydrophobic core. Fig. 4 shows the distribution (number of segments per unit length) of terminal ( $\text{CH}_3$ ) groups, double bonded carbons ( $-\text{CH}=\text{}$ ) and the sum of all methylene ( $-\text{CH}_2-$ ) segments comprising the two hydrophobic tails of dioleoyl phosphatidyl choline (DMPC). The lipid tail of these molecules is composed of two  $-(\text{CH}_2)_7-(\text{CH}=\text{CH})-(\text{CH}_2)_7-\text{CH}_3$  chains. One set of curves represents experimental results obtained by X-ray and Neutron scattering [49–50]. The other represents the predictions of the mean field theory [26]. The thickness of the hydrophobic region, defined as the average distance between the lipid carbonyl groups on opposite interfaces of the membrane, is  $d = 32 \text{ \AA}$ . The agreement between the measured and calculated results is satisfactory, at least with respect to the peaks of the various segment distributions. The main difference appears in the width of the  $\text{CH}_2$  distribution, showing wider 'wings' of the experimental results. Yet, it should be noted that no attempts were made to fit the calculated results to experiment. The only input into the calculation was the thickness of the membrane allowing, as in other calculations of this kind, for small fluctuations of the lipid head group around the hydrocarbon–water interface. Further details of this and other calculations are discussed in Ref. [26].

The mean field theory has been used to calculate various other single chain properties of interest. For instance, the average lateral fluctuations of lipid chain segments. Here

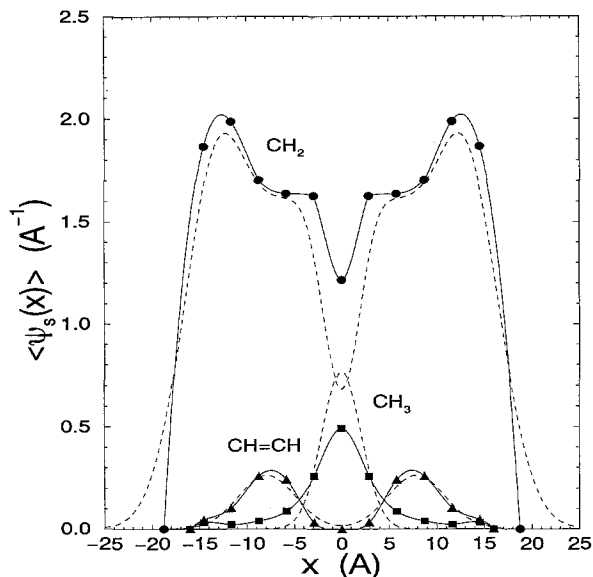


Fig. 4. The distribution of lipid chain segments across a POPC bilayer (adapted from [26]). ●, ■ and ▲ represent the results calculated by the mean field theory for the (sum of all) CH<sub>2</sub> segments, CH<sub>3</sub> groups and CH=CH groups, respectively [26]. The dashed lines are the experimental results [50].

too, good agreement with experiment was found [26].

#### 4. A lipid–protein interaction model

A hydrophobic “solute”, such as the hydrophobic part of an integral protein, modifies the conformational properties of the lipids around it. In general this ‘perturbation’ raises the free energy of the surrounding lipids, so that when two or more hydrophobic inclusions are in close proximity to each other the, lipid-mediated, interaction between them is attractive, thus favoring solute aggregation. The driving force for this aggregation is the tendency to minimize the contact area, and hence the extent of lipid perturbation, between the hydrophobic solutes and their surrounding lipid chains.

Many theoretical models have been proposed to describe and calculate the effects of an integral protein, usually treated as a rigid hydrophobic perturbation, on the lipid environment [7,15,51–62]. Only very few models have considered the lipid–protein interaction on a molecular level. One such model, based on the molecular theory presented in Section 2, is outlined in this section [7].

We use  $d_L^0$  to denote the thickness of the lipid hydrophobic core. It is commonly assumed that when a rigid protein (or another inclusion) of hydrophobic thickness  $d_P \sim d_L^0$  is incorporated into the membrane, the flexible lipid chains around it will adjust their length so as to shield the protein from direct contact with the surrounding water; see Fig. 5. Using  $d_L(x)$  to denote the bilayer thickness at a distance  $x$  from the

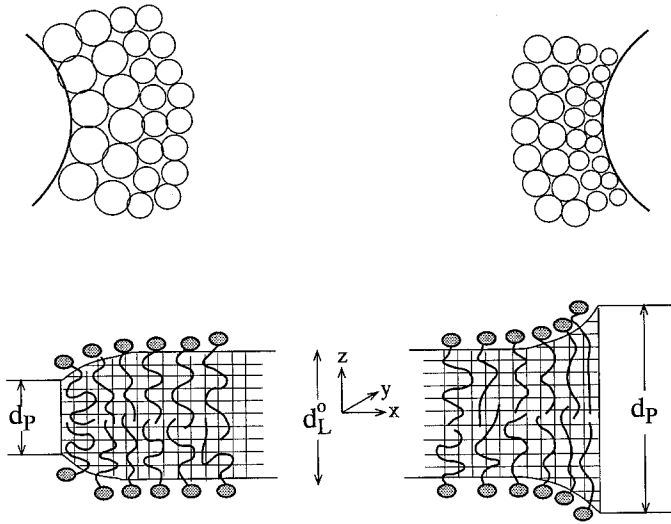


Fig. 5. Schematics of the lipid–protein interaction model described in the text (adapted from [7]). At the bottom is a ‘side view’ of the bilayer, depicting the protein as a rigid wall of thickness  $d_p$ , either larger (right, ‘positive mismatch’) or smaller (left, ‘negative mismatch’) than the unperturbed bilayer thickness  $d_L^0$ . The chains in the vicinity of the protein are either stretched (when  $d_p > d_L^0$ ) or compressed (when  $d_p < d_L^0$ ) in order to bridge over the hydrophobic mismatch. At the top is a ‘top view’ of the membrane illustrating the corresponding changes in the average cross-sectional area per chain as a function of the distance from the protein.

protein, this assumption implies  $d_L(0) = d_p$ . The variation of  $d_L(x)$ , between  $d_p$  at  $x = 0$  to  $d_L^0$  at  $x \rightarrow \infty$ , will be modeled as

$$d_L(x) = d_L^0 + (d_p - d_L^0) \exp(-x/\xi), \quad (23)$$

with  $\xi$  measuring the range (or the ‘coherence length’) of the perturbation. The difference  $d_p - d_L^0$  will be referred to as *the hydrophobic mismatch*. The model treats  $\xi$  as a variational parameter whose value is determined by minimization of the total perturbation free energy. The exponential variation of the membrane thickness profile, (23), has been derived by some of the Landau-type theories of lipid–protein interaction [58–59]. Yet, in the present model it is used as a convenient parametrization of  $d_L(x)$ . In fact, some of the continuum elastic theories of lipid–protein interaction predict more complicated, including non-monotonic, functional forms for  $d_L(x)$  [54–56].

The model described in Fig. 5 treats the protein as a rigid cylinder embedded in the membrane. The diameter,  $D$ , of the cylinder cross section is assumed to be considerably larger than the average lateral dimension of the lipid chains, i.e.  $D \gg a^{1/2}$  where  $a$  is the average cross-sectional area per chain. Accordingly, to the lipids in its periphery the protein appears as a planar wall. Free energy calculations have been performed assuming that the protein wall is flat and extending normally and symmetrically around the bilayer midplane [7]. Other geometries, e.g. a conical inclusion, can be treated similarly.

We choose the protein wall to be parallel to the  $zy$ -plane ( $z$  is the direction normal to the membrane plane), the lipid–protein interaction free energy, per unit length of the protein perimeter (along the  $y$ -direction) is given by

$$\Delta F = 2 \int dx [\sigma(x)f(x) - \sigma^0 f^0], \quad (24)$$

where  $f(x)$  is the local free energy per molecule at distance  $x$  from the protein and  $\sigma(x)dxdy$  is the number of molecules originating from a small area element  $dxdy$  of one of the two membrane interfaces. (More precisely,  $dxdy$  is the projection of this area element onto the bilayer midplane).  $\sigma^0$  and  $f^0$  are the corresponding quantities for the unperturbed membrane that is,  $\sigma^0 = \sigma(x)$  and  $f^0 = f(x)$  as  $x \rightarrow \infty$ . The factor 2 in front of the integral accounts for the two leaflets of the bilayer.

The head group surface density in the planar bilayer is  $\sigma^0 = 1/a^0$ , where  $a^0 = 2v/d_L^0$  is the average area per chain;  $v$  denoting the volume of the hydrophobic tail. Assuming, as before, that the hydrophobic core is uniform and liquid-like, we have  $\sigma(x) = 2v/d_L(x)$ . Note, however, that except for the planar bilayer  $\sigma(x) \neq 1/a(x)$ , where  $a(x)$  is the average local interface area per chain in the vicinity of the protein. This latter quantity is given by

$$a(x) = \frac{2v}{d_L(x)} \left\{ 1 + \frac{1}{4} \left( \frac{\partial d_L(x)}{\partial x} \right)^2 \right\}^{1/2}. \quad (25)$$

The free energy per molecule can be expressed as a sum of tail, surface and head group contributions, (see Section 2)

$$f(x) = f_t(x) + f_s(x) + f_h(x). \quad (26)$$

The tail free energy and the corresponding spd are given by Eqs. (13) and (14), respectively; with  $s \rightarrow x$  and  $r \rightarrow (x, z)$ . The numerical calculation of  $f_t(x)$  is considerably more complex than in the planar bilayer case, since  $\lambda = \lambda(x, z)$  varies along both  $x$  and  $z$  whereas for the planar bilayer  $\lambda \rightarrow \pi(z)$  is only a function of  $z$ . Nevertheless, the calculations are feasible and representative numerical results will be shown below. In these calculations the surface free energy is modeled as  $f_s = \gamma a(x)$  with  $\gamma = 0.12 \text{ kT}/\text{\AA}^2$ , and  $f_h(x)$  is represented by the simple form  $f_h(x) = C/a(x)$  with  $a(x)$  given by (25). The parameter  $C$  was chosen such that for a planar bilayer composed of  $C_{14}$  ( $\mathcal{P}-(\text{CH}_2)_{13}-\text{CH}_3$ ) lipids the equilibrium area per chain is  $a_0 \cong 32 \text{ \AA}^2$ ; see Fig. 2.

The lipid–protein interaction free energy  $\Delta F$  of the  $C_{14}$  bilayer is shown in Fig. 6 for three choices of the head group interaction parameter;  $C = 48 \text{ kT}$ ,  $12 \text{ kT}$  and  $0$ . First we note that  $\Delta F \neq 0$  even for the case of no hydrophobic mismatch, when  $d_P = d_L^0$ . In this case there is no contribution to  $\Delta F$  from the surface ( $\Delta F_s = 0$ ) or head group ( $\Delta F_h = 0$ ) terms; only  $\Delta F_t > 0$ . Even though there is no change in the average chain length, the presence of the impenetrable protein wall reduces the conformational freedom of nearby chains, resulting in excess chain orientational ordering and non-negligible

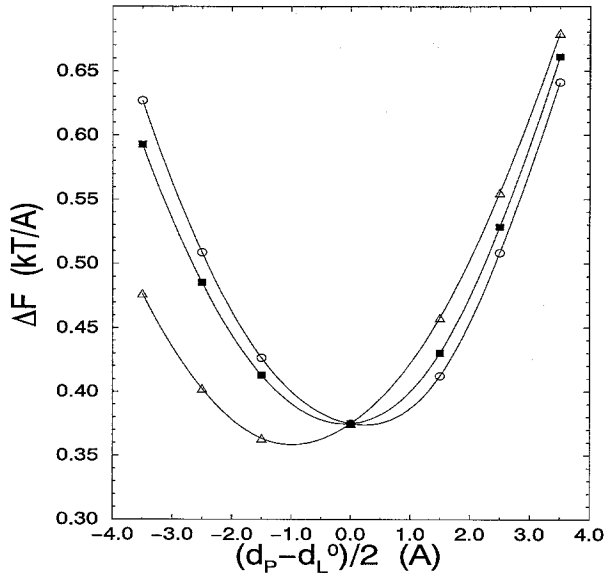


Fig. 6. The lipid-protein interaction free energy (per unit length of perimeter length) for a bilayer of  $C_{14}$  chains, as a function of the hydrophobic mismatch (adapted from [7]). ○, ■ and △ correspond to three different choices of the head group repulsion strength,  $C = 0, 12, 48$  kT, respectively.

positive contribution to  $F_t$ . These notions are confirmed by explicit calculations of bond orientational order parameter profiles, showing increased  $\langle S_k \rangle$  values for chains near the protein, as compared to those away from it [7]. The chain conformational calculations also show a finite (though small) average tilt angle of the chains (away from the wall). It should be noted that the first molecular model of lipid-protein interaction, that was proposed by Marcelja, has been formulated for the  $d_P = d_L^0$  case [15]. In Marcelja's model, like in the one presented here,  $\Delta F_t > 0$  due to the loss of lipid chain conformational freedom in the protein vicinity [15].

When  $d_P > d_L^0$  the lipid tails are stretched beyond their length in the unperturbed membrane, resulting in  $\Delta F_t > 0$ . In parallel, the average area per head group decreases [22] and consequently  $\Delta F_s < 0$ . The opposite behavior characterizes the case  $d_P < d_L^0$ . The contribution of head group repulsion ( $\Delta F_h$ ) to  $\Delta F$  is, at least according to the model described, small compared to  $\Delta F_s$  and  $\Delta F_t$ . Thus, since as  $d_P - d_L^0$  increases  $\Delta F_t$  increases whereas  $\Delta F_s$  decreases, the minimum of  $\Delta F = \Delta F_t + \Delta F_s + \Delta F_h \simeq \Delta F_t + \Delta F_s$  is generally around  $d_P - d_L^0 = 0$ . However, as seen in Fig. 6, the minimum of  $\Delta F$  shifts to a negative  $d_P - d_L^0$  value when the strength of head group repulsion increases. In other words, negative hydrophobic mismatch can in fact relieve some of the lipid-protein interaction free energy when head repulsion is strong. Similarly, positive mismatch can reduce  $\Delta F$  (compared to the case  $d_P = d_L^0$ ) in the case of strong chain repulsion. This effect has recently been predicted by Safran and Dan using a continuous elastic theory for the effect of hydrophobic inclusions on membrane properties [55–56]. Its origin, according to their analysis, is the nonzero spontaneous curvature of the monolayers

comprising the bilayer. To understand the effect it is worthwhile to elaborate on the role of spontaneous curvature in lipid bilayers.

Consider one of the two monolayers comprising a lipid bilayer and assume it is planar. The three forces, head group repulsion, surface tension and chain repulsion, balance each other at some equilibrium area per chain,  $a_{eq}$ . These forces also exert moments which may prefer a finite “spontaneous” curvature for the monolayer. The curvature may be either positive (the hydrocarbon–water interface convex towards the water), negative or zero. Large moments of head group repulsion will tend to induce positive spontaneous curvature. Large moments of chain repulsion will act in the opposite direction. When two monolayers are brought into contact to form a planar bilayer, both are ‘frustrated’ energetically since their curvature is not the optimal (spontaneous) one. Yet, the planar bilayer geometry usually involves the least curvature energy cost for the two monolayers. Now, suppose that head group repulsion is strong enough to favor positive spontaneous curvature for the monolayer. If  $d_P < d_L^0$  then the lipids around the protein wall are packed with positive spontaneous curvature (see Fig. 5), thus relieving some of the frustration energy associated with the formation of the planar bilayer. The case  $C = 48$  kT in Fig. 6 corresponds to strong head group repulsion and hence positive spontaneous curvature. Indeed, we note that for this case the minimum in  $\Delta F$  takes place at a negative value of  $d_P - d_L^0$ . Similarly, stronger chain repulsion would shift the minimum towards positive  $d_P - d_L^0$ .

Many other structural and thermodynamic characteristics of the lipid–protein bilayer can be derived from the model described in this section. One result of particular interest is the spatial range of the perturbation,  $\xi$ . The perturbation of lipid order by the protein wall extends to  $\sim 3\xi$ . The calculations show that  $\xi \sim 5$  Å. Since, typically, the lateral dimension of a lipid chain is  $a^{1/2} \simeq (5-6)$  Å, it follows that the range of perturbation corresponds to just a few molecular diameters.

## 5. The vesicle–micelle transition

Lipid molecules in aqueous solution self-assemble spontaneously into extended 2D bilayers. The spontaneous (equilibrium, minimal free energy) curvature of bilayers is generally zero, i.e. they tend to be planar. To avoid the excess free energy associated with the exposure of their edges to water, the bilayers often close on themselves to form vesicles, at least in dilute solutions [63]. At higher lipid concentrations they may organize in multilamellar structures [63,64]. Other, non-lipid, amphiphiles which in dilute solution self-assemble into high curvature aggregates such as cylindrical micelles, usually organize in multi-lamellar phases at higher concentration. These phases are stabilized by inter-aggregate interactions which overcome the intrinsic preference of the molecules to pack in highly curved aggregates.

Surfactant molecules, such as octylglucoside or bile salts, form micelles in dilute solution, reflecting their high spontaneous curvature [65,66]. Recall that any point of a curved surface can be characterized by two local principal curvatures,  $c_1$  and

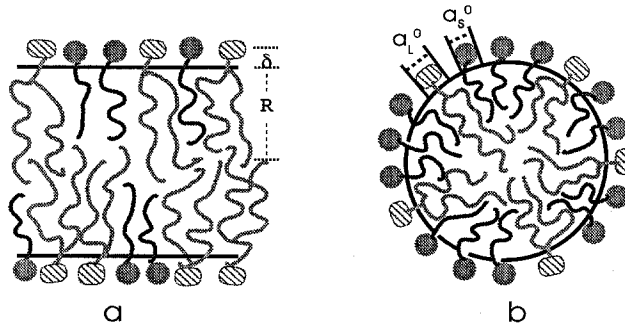


Fig. 7. A mixed lipid surfactant bilayer (a) and a mixed micelle (b) (adapted from [27]).  $a_L^0$  and  $a_S^0$  are the bare head group areas of the two amphiphilic components,  $\delta$  is the distance from the plane of head group repulsion to the hydrocarbon–water interface.

$c_2$ , with  $R_i = 1/c_i$  ( $i = 1, 2$ ), denoting the corresponding radius of curvature. Thus, for example, the hydrocarbon–water interface of a spherical micelle of radius  $R$  is everywhere characterized by  $c_1 = c_2 = 1/R$ , with  $R \leq l$  where  $l$  is the length of the fully extended amphiphile tail. Similarly, in cylindrical micelles (except at the hemispherical caps),  $c_1 = 1/R_1$  whereas  $c_2 = 0$ ;  $R_1$  denoting the radius of the cylinder cross section ( $R_1 \leq l$ ) and  $R_2 \rightarrow \infty$  denoting the radius of the cylinder axis. In planar bilayers  $c_1 = c_2 = 0$  and in spherical vesicles of radius  $R$ ,  $c_1 = c_2 = 1/R$  with  $R \gg l$ .

Consider now a dilute binary aqueous solution containing lipids, whose spontaneous aggregation geometry is planar ( $c_1 = c_2 \simeq 0$ ), and surfactants which in dilute solution prefer organization in, say, cylindrical micelles ( $c_1 \cong 1/l$ ,  $c_2 = 0$ ). Let  $\chi = \chi_L = N_L/(N_L + N_S) = N_L/N$  denote the mole fraction of lipids and  $\chi_S = 1 - \chi$  the mole fraction of surfactants in solution;  $N_L$  and  $N_S$  denoting the number (or concentration) of lipid and surfactant molecules, respectively. (The mole fractions involve only the amphiphilic components, not the solvent,  $\chi_S + \chi_L = 1$ ). In the limits  $\chi = 1$  and  $\chi = 0$  the amphiphiles form lipid vesicles ( $c_1 = c_2 \simeq 0$ ) and surfactant micelles, respectively. When a small amount of surfactant molecules is added to a system composed of lipid vesicles, a certain fraction of them (typically very small, corresponding to the cmc (critical micellar concentration) [1,3–5]) are dispersed as monomers in the solution, the rest are incorporated (‘solubilized’) into the vesicles. As in ordinary binary mixtures, the thermodynamic driving force for the incorporation of the surfactant into the lipid bilayer is the mixing entropy, which overcounts the tendency of the surfactant and lipid molecules to pack, separately, according to their energetically preferred aggregation geometries. Similarly, upon adding small amounts of lipids to a surfactant-rich system they will be solubilized in the surfactant micelles (hardly any of them will be present as monomers, due to the extremely low cmc of lipids). Schematic illustrations of a mixed lipid–surfactant bilayer and a mixed cylindrical micelle are shown in Fig. 7.

In ordinary binary molecular solutions, say of  $A$  and  $B$  molecules, phase separation of an  $A$ -rich and a  $B$ -rich phase can take place, provided the effective  $A$ – $B$  interaction:  $w = w_{AB} - (w_{AA} + w_{BB})/2$  is repulsive, i.e.  $w > 0$ ;  $w_{IJ}$  ( $I = A, B$ ) denotes the interaction

energy between  $I$  and  $J$  molecules (integrated over distances and orientations or, in lattice models, between neighboring molecules). More precisely, phase separation occurs below a certain critical temperature  $T_c$  (proportional to  $w$ ), and only over a certain range of (intermediate) compositions, which broadens as  $T$  decreases farther from  $T_c$ .

An analogous scenario can, and usually does, happen in aqueous solutions of lipids and surfactants. The analogue of  $w$  in these systems is the difference in the packing (free) energy of surfactants and lipids in a mixed system, compared to their packing in separate aggregates. The coexisting phases in lipid–surfactant solutions, if and when phase separation takes place, are vesicles with amphiphile composition  $x_v$  ( $v$  = vesicle) and micelles with composition  $x_m$  ( $m$  = micelle), such that  $x_m < x_v$ . The separated phases appear in different regions of space (vesicles and micelles floating in the aqueous solution) and are characterized by very different symmetries: nearly planar lipid–rich bilayer vesicles vs. elongated (or sometimes globular) surfactant–rich micelles.

This qualitative thermodynamic scenario does indeed take place in many lipid–surfactant systems [67–72] and is of considerable biological importance, e.g. for membrane reconstitution [66]. What typically happens is that a lipid vesicle can take up surfactant molecules up to a limit corresponding to a lipid content  $x_v$ . Beyond that limit the vesicles break into micelles with lipid content  $x_m$ . In lecithin–bile salt and lecithin–octylglucoside mixtures the compositions of coexisting vesicles and micelles are about  $x_v \sim 1/2$  and  $x_m \sim 1/4$ .

A theoretical model of the vesicle–micelle transition has recently been formulated by Andelman, Kozlov and Helfrich [73]. These authors have expressed the free energy, of both the (mixed) bilayer and micelle, as a sum of a curvature energy term and a mixing entropy term. The average (Helmholtz) free energy per molecule in each of the two aggregation geometries was written as

$$\psi(x) = \frac{1}{2}\kappa[c_1 + c_2 - c_0(x)]^2 + kT[x \ln x + (1-x) \ln(1-x)], \quad (27)$$

with  $x$  denoting the lipid mole fraction in the aggregate. (Actually in [73]  $x$  denotes the area fraction of lipids, measured at the hydrocarbon–water interface. This difference is irrelevant for the present discussion and for understanding this phenomenon). The second term in (27) is an ideal mixing entropy contribution. The first term is the common, Helfrich, form of the bending free energy of a membrane [32].  $\kappa$  denotes the curvature (splay) elastic modulus and  $c_0(x)$  is the spontaneous curvature of an aggregate with composition  $x$ . The spontaneous curvature has been assumed to vary linearly with  $x$ , say from  $c_0(x=0) = 1/R$  corresponding to a cylindrical surfactant micelle of radius  $R$ , to  $c_0(x=1) = 0$  corresponding to a planar lipid bilayer (or very large vesicle).  $\kappa$  was treated as a constant, independent of  $x$  or aggregation geometry. Then  $f(x)$  is calculated for the vesicle ( $c_1 = c_2 \simeq 0$ ) and for the cylindrical micelle ( $c_1 = 1/R, c_2 = 0$ ), and by equating the chemical potentials of the lipid and surfactant in the two geometries (common tangent construction), a general expression can be derived for the lipid composition of the vesicle and micelle at the transition.

The above model can predict some interesting qualitative trends, e.g. the dependence of the coexisting compositions on  $c_0(x), T$  and  $\kappa$ . Yet it must be remembered that

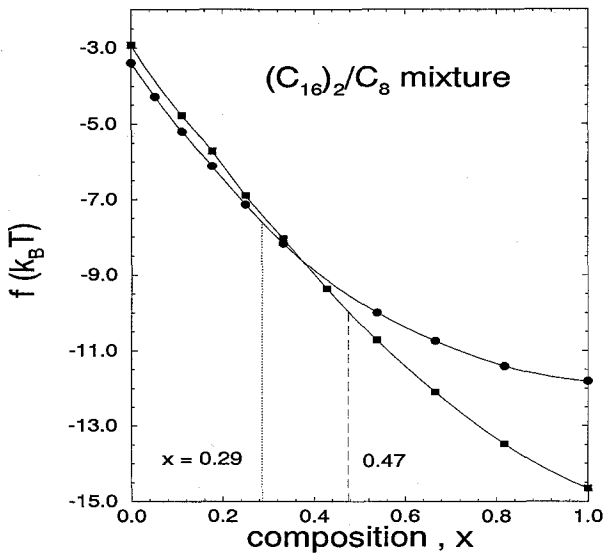


Fig. 8. Average free energy per molecule in a mixed  $(C_{16})_2/C_8$  lipid surfactant bilayer (■) and cylindrical micelle (●), as a function of lipid mole fraction (adapted from [27]). The compositions of the bilayer ( $x = 0.47$ ) and micelle ( $x = 0.29$ ), at the vesicle–micelle transitions are evaluated by common tangent construction (corresponding to equating the chemical potentials of each component in both aggregation geometries).

the bending energy term in (27) is valid only for small deviations, mainly of planar films, around the equilibrium curvature. Vesicles and cylindrical micelles correspond to very different equilibrium curvatures. It is highly unlikely that the harmonic (quadratic) form of the bending energy, with the same  $\kappa$  for all geometries can faithfully describe the geometry dependence of the amphiphile packing free energy. Furthermore, molecular calculations of  $\kappa$  show that it depends sensitively on  $x$  [6,74]. (For instance, the bending rigidity of lipid membranes decreases rapidly upon adding short chain surfactants to the bilayer). Interestingly enough, recent calculations of this kind show that in some mixtures  $c_0(x)$  varies nearly linearly with  $x$  over a wide range of composition [74].

In view of the above notions we have replaced the elastic energy in (27) by the expressions corresponding to the molecular mean field theory described in Sections 2–4. Thus, instead of (27) we write

$$\psi_g(x) = x f_g^L(x) + (1-x) f_g^S(x) + kT [x \ln x + (1-x) \ln(1-x)], \quad (28)$$

with  $f_g^L(x)$  denoting the packing free energy per lipid molecule in a mixed aggregate of geometry  $g$  ( $g = \text{vesicle, micelle}$ ) and composition  $x$ . Then, plotting  $\psi_g(x)$  vs.  $x$  for the two aggregation geometries one can evaluate the coexisting compositions,  $x_v$  and  $x_m$ , using common tangent construction.

The results of one calculation of this kind, corresponding to a given set of molecular parameters (see below) are shown in Fig. 8. Also marked on the figure is the composition  $x_v = 0.47$  below which the vesicle is unstable, and the composition  $x_m = 0.29$  of the

micelles formed when the vesicles break. Conversely,  $x_m$  is the maximal lipid content in a cylindrical micelle, beyond which vesicles of composition  $x_v$  begin to form.

The results shown in Fig. 8 as well as several additional cases are discussed in more detail elsewhere [27]. Here, we shall only mention the basic assumptions. The system considered is a mixture of saturated double chain lipids  $\mathcal{P}_L-[(\text{CH}_2)_{15}-\text{CH}_3]_2$  and short single chain surfactants  $\mathcal{P}_S-(\text{CH}_2)_7-\text{CH}_3$ , with  $\mathcal{P}_L$  and  $\mathcal{P}_S$  denoting the lipid and surfactant head groups, respectively. As in previous sections, the free energy of the mixed bilayer, and the mixed cylinder, has been expressed as a sum of tail ( $f_t$ ) surface ( $f_s = \gamma a$ ) and head group contributions. The head group contribution to  $x f_g^L(x) + (1-x) f_g^S(x)$  has been modeled as a steric repulsion free energy [38]

$$f_h^g = -kT \ln(1 - a_h/\bar{a}^g). \quad (29)$$

Here  $\bar{a}^g = \bar{a}^g(x)$  is the average area per head group in aggregates of geometry  $g$  ( $g = v, m$ ). This area is measured at the plane of head group repulsion, assumed to be located at distance  $\delta$  from the hydrocarbon–water interface. For a planar bilayer (large vesicle)  $\bar{a}^v = a^v$ , where  $a^v$  is the area per head group at the interface; for a cylinder micelle of radius  $R$ ,  $\bar{a}^m = a^m(1 + \delta/R)$ . The quantity  $a_h = a_h(x) = x a_h^L + (1-x) a_h^S$  is the average bare (hard core) head group area per molecule, at the plane of head group interactions.  $a_h^L$  and  $a_h^S$  denote, respectively, the bare head group areas per lipid and surfactant molecule.

The surface contribution to the free energy is modeled as

$$f_s^g(x) = x\gamma(a^g - a_h^L) + (1-x)\gamma(a^g - a_h^S) = \gamma(a^g - a_h). \quad (30)$$

The chain conformational contributions were calculated using the mean field theory for mixed systems, as outlined in Section 2.

The numerical values used for the specific calculation shown in Fig. 8 were  $\gamma = 0.12$   $\text{kT}/\text{\AA}^2$ ,  $a_h^L = 42$   $\text{\AA}^2$ ,  $a_h^S = 50$   $\text{\AA}^2$  and  $\delta = 1.1$   $\text{\AA}$ . The choice of  $a_h^L$  ensures that the equilibrium average cross-sectional area per molecule in a pure lipid bilayer is  $68$   $\text{\AA}^2$ , as commonly found for lecithin bilayers [69]. The numerical values of  $a_h^S$  and  $\delta$  (which in Ref. [27] were treated as parameters controlling the spontaneous curvature of the surfactant) ensure that the optimal packing geometry of the  $\text{C}_8$  surfactant molecules in dilute solution is a cylindrical micelle, with an average area per surfactant head group  $a \simeq 55$   $\text{\AA}^2$ .

The free energy per molecule has been calculated as a function of composition  $x$ , for both geometries, and the values of the amphiphile in the vesicles and the micelles, at the transition ( $x_v = 0.47$  and  $x_m = 0.29$ ) were determined by common tangent construction. These values for  $x_v$  and  $x_m$  are in the range observed experimentally [69–72]. The molecular parameters used ( $a_h^L, a_h^S, \gamma, \delta$ ) are all very reasonable and, moreover, have been adjusted so as to ensure micelle formation at  $x \rightarrow 0$  and vesicle formation at  $x \rightarrow 1$ . Nevertheless, it must be mentioned that the uncertainties involved in choosing these parameters are considerable. Different choices of, say,  $a_h^L$  and  $\delta$ , can lead to substantial shifts in the values inferred for  $x_v$  and  $x_m$ . The semi-empirical adjustment of such parameters by referring to limiting (i.e. the pure) cases seems, at present, as

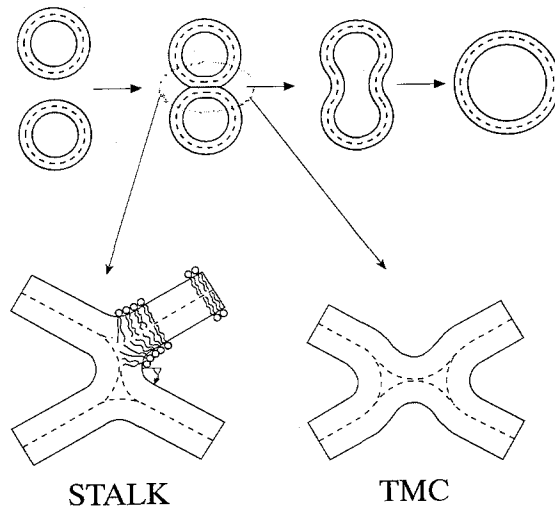


Fig. 9. Schematic illustration of the several stages in the fusion of vesicle bilayers (top). The bottom figure shows in more detail two of the proposed structural intermediates along the fusion pathway [76,75].

the most plausible procedure. Notwithstanding these reservations the model described in this section does account for the basic interactions and trends characteristic of the vesicle–micelle transition. Other structural transitions, such as from lamellar to inverted hexagonal or cubic phases, can possibly be accounted for using a similar approach.

## 6. Concluding remarks

In systems of low symmetry such as the lipid–protein membrane, the molecular mean field theory described in this chapter requires some nontrivial calculations. Nevertheless, the computational effort involved is still substantially lesser than that required in large scale computer simulations. Various other systems and processes in membrane biophysics can be studied and analyzed, on a molecular level, using this approach. These include, for example, the thermodynamic stability of mixed vesicles, pore (and other defect) formation in membranes or the phase transition from lamellar to inverted hexagonal phases. Let us conclude this section by mentioning some very preliminary results concerning an issue of considerable biological relevance: the fusion of lipid vesicles.

Several authors have proposed phenomenological models for the mechanism and the structural intermediates involved in the process of membrane fusion [75–77], after the initial adhesion stage [78–79]. One of the suggested pathways, the ‘modified Stalk mechanism’ suggested by Siegel [75], is schematically illustrated in Fig. 9. Siegel has also estimated the excess free energies associated with the formation of the structural intermediates, using the continuum theory for membrane curvature and stretching elasticity [32].

We have recently performed calculations of the kind described in Sections 2 and 3, for the excess free energy of the ‘Stalk’ intermediate (Fig. 9), for a pure lipid membrane composed of  $C_{14}$  chains. The results obtained are  $\Delta F \sim 100$  kT. These numbers are in surprisingly good agreement with those obtained using the continuum theory. The agreement is surprising because the structural intermediates involve variations of packing geometry extending over only few molecular diameters. However, additional calculations are called for before this good agreement can be confirmed.

## Acknowledgements

We would like to thank E. Sackmann, W.M. Gelbart, I. Szleifer, D. Lichtenberg, Y. Barenholz, D. Andelman, Y. Talmon, S. Safran, M. Kozlov and D. Siegel for helpful discussions and comments on the topics outlined in this chapter. The financial support of the National Science Foundation administered by the Israel Academy of Science and Humanities and the Yeshaya Horowitz Association is gratefully acknowledged. The Fritz Haber Research Center, where this research was done, is supported by the Minerva Gesellschaft für die Forschung, mbH, Munich Germany.

## References

- [1] A. Ben-Shaul and W.M. Gelbart, in: W.M. Gelbart, A. Ben-Shaul and D. Roux, Eds., *Micelles, Membranes, Microemulsions and Monolayers*, Ch. 1 (Springer, New York, 1994).
- [2] A. Ben-Shaul, in: R. Lipowsky and E. Sackmann, Eds., *Handbook of Physics of Biological Systems*, Vol. 1, Ch. 7 (Elsevier, Amsterdam, 1995).
- [3] C. Tanford, *The Hydrophobic Effect*, 2nd ed. (Wiley-Interscience, New York, 1980).
- [4] J.N. Israelachvili, *Intermolecular and Surface Forces* (Academic, London, 1985).
- [5] H. Wennerström and B. Lindman, *Phys. Rep.* 52 (1979) 1.
- [6] I. Szleifer, D. Kramer, A. Ben-Shaul, W.M. Gelbart and S.A. Safran, *J. Chem. Phys.* 92 (1990) 6800.
- [7] D.R. Fattal and A. Ben-Shaul, *Biophys. J.* 65 (1993) 1795.
- [8] M.A. Carignano and I. Szleifer, *J. Chem. Phys.* 98 (1993) 5006.
- [9] H. Heller, M. Schaefer and K. Schulten, *J. Phys. Chem.* 97 (1993) 8343.
- [10] E. Egberts, S.J. Marrink and H.J.C. Berendsen, *Eur. Biophys. J.* 22 (1994) 423.
- [11] S.J. Marrink, M. Berkowitz and H.J.C. Berendsen, *Langmuir* 9 (1993) 3122.
- [12] H.L. Scott and S.L. Cherng, *Biochim. Biophys. Acta* 510 (1978) 209.
- [13] J.H. Ipsen, K. Jørgensen and O.G. Mouritsen, *Biophys. J.* 58 (1990) 1099.
- [14] S. Marčelja, *Biochim. Biophys. Acta* 367 (1974) 165.
- [15] S. Marčelja, *Biochim. Biophys. Acta* 455 (1976) 1.
- [16] See, e.g., P.G. de Gennes and J. Prost, *The Physics of Liquid Crystals*, 2nd ed. (Clarendon, Oxford, 1993).
- [17] K.A. Dill and P. Flory, *Proc. Natl. Acad. Sci. USA* 77 (1980) 3115.
- [18] K.A. Dill and D. Stigter, *Biochem. J.* 27 (1988) 3446.
- [19] D.W.R. Gruen, *J. Phys. Chem.* 89 (1985) 146.
- [20] D.W.R. Gruen, *Prog. Colloid Polymer Sci.* 70 (1985) 6.
- [21] A. Ben-Shaul, I. Szleifer and W.M. Gelbart, *J. Chem. Phys.* 83 (1985) 3597.
- [22] I. Szleifer, A. Ben-Shaul and W.M. Gelbart, *J. Chem. Phys.* 83 (1985) 3612.
- [23] I. Szleifer, A. Ben-Shaul and W.M. Gelbart, *J. Chem. Phys.* 86 (1987) 7094.
- [24] I. Szleifer, A. Ben-Shaul and W.M. Gelbart, *J. Chem. Phys.* 85 (1986) 5345.
- [25] I. Szleifer, A. Ben-Shaul and W.M. Gelbart, *J. Phys. Chem.* 94 (1990) 5081.

- [26] D.R. Fattal and A. Ben-Shaul, *Biophys. J.* 67 (1994) 983.
- [27] D.R. Fattal, D. Andelman and A. Ben-Shaul, *Langmuir* 11 (1995) 1154.
- [28] F.A.M. Leermakers and J.M.H.M. Scheutjens, *J. Chem. Phys.* 89 (1988) 3264.
- [29] P.A. Barneveld, D.E. Hesselink, F.A.M. Leermakers, J. Lyklema, and J.M.H.M. Scheutjens, *Langmuir* 10 (1994) 1084.
- [30] L.A. Meijer, F.A.M. Leermakers and A. Nelson, *Langmuir* 10 (1994) 1199.
- [31] P.J. Flory, *Statistical Mechanics of Chain Molecules* (Wiley-Interscience, New York, 1969).
- [32] W. Helfrich, *Z. Naturforsch. C* 28 (1973) 693; *C* 29 (1974) 510.
- [33] E.A. Evans and R. Skalak, in: *Critical Reviews in Bioengineering* (CRC, Boca Raton, 1979) p. 181.
- [34] A.G. Petrov and I. Bivas, *Prog. Surf. Sci.* 16 (1984) 389.
- [35] D.D. Lasic, *Biochem. J.* 256 (1988) 1.
- [36] D. Stigter, J. Mingins and K.A. Dill, *Biophys. J.* 61 (1992) 1616.
- [37] D. Andelman, in: R. Lipowsky and E. Sackmann, Eds., *Handbook of Physics of Biological Systems*, Vol. 1 (Elsevier, Amsterdam, 1995).
- [38] S. Puvvada and D. Blankschtein, *J. Phys. Chem.* 96 (1992) 5579; R. Nagarajan, *Langmuir* 1 (1985) 331.
- [39] G. Cevc, *Biochim. Biophys. Acta* 1031 (1990) 311.
- [40] J. Ennis, *J. Chem. Phys.* 97 (1992) 663.
- [41] M. Winterhalter and W. Helfrich, *J. Phys. Chem.* 96 (1992) 327.
- [42] D.J. Mitchell and B.W. Ninham, *Langmuir* 5 (1989) 1121.
- [43] H.N.W. Lekkerkerker, *Physica A* 159 (1989) 319.
- [44] J. Seelig and N. Waespe-Sarčević, *Biochem. J.* 17 (1978) 3310.
- [45] J. Seelig and A. Seelig, *Quart. Rev. Biophys.* 13 (1980) 19.
- [46] M. Bloom, E. Evans and O.G. Mouritsen, *Q. Rev. Biophys.* 24 (1991) 293.
- [47] J.F. Nagle, *Biophys. J.* 64 (1993) 1476.
- [48] O. Edholm, *Chem. Phys.* 64 (1982) 259.
- [49] M.C. Wiener and S.H. White, *Biophys. J.* 61 (1992) 428.
- [50] M.C. Wiener and S.H. White, *Biophys. J.* 61 (1992) 434.
- [51] J.R. Abney and J.C. Owicki, in: A. Watts and J.J.H.M. de Pont, Eds., *Progress in Protein-Lipid Interactions* (Elsevier, Amsterdam, 1985) p. 1.
- [52] O.G. Mouritsen and M. Bloom, *Ann. Rev. Biophys. Biomol. Struct.* 22 (1993) 145.
- [53] H.W. Huang, *Biophys. J.* 50 (1986) 1061.
- [54] P. Helfrich and E. Jakobsson, *Biophys. J.* 57 (1990) 1075.
- [55] N. Dan, P. Pincus and S.A. Safran, *Langmuir* 9 (1993) 2768.
- [56] N. Dan and S.A. Safran, *Israel J. Chem.* 35 (1995) 37.
- [57] A. Caillé, D. Pink, F. De Verteuil and M.J. Zuckermann, *Can. J. Phys.* 58 (1980) 581.
- [58] J.C. Owicki and H.M. McConnell, *Proc. Natl. Acad. Sci. USA* 76 (1979) 4750.
- [59] F. Jähnig, *Biophys. J.* 36 (1981) 329.
- [60] F. Jähnig, H. Vogel and L. Best, *Biochem. J.* 21 (1982) 6790.
- [61] H.L. Scott and T.J. Coe, *Biophys. J.* 42 (1983) 219.
- [62] O.G. Mouritsen and M. Bloom, *Biophys. J.* 46 (1984) 141.
- [63] D.D. Lasic, *Liposomes: From Physics to Applications* (Elsevier, Amsterdam, 1993).
- [64] W.M. Gelbart, A. Ben-Shaul and D. Roux, Eds., *Micelles, Membranes, Microemulsions and Monolayers* (Springer, New York, 1994).
- [65] P. Rosevear, T. VanAken, J. Baxter and S. Ferguson-Miller, *Biochem. J.* 19 (1980) 4108; T. VanAken, S. Foxall-VanAken, S. Casetleman and S. Ferguson-Miller, *Methods in Enzymology* 125 (1986) 27.
- [66] R.B. Jennis, *Biomembranes: Molecular Structure and Function* (Springer, New York, 1989).
- [67] P. Shurtenberger, N. Mazer and W. Känzig, *J. Phys. Chem.* 89 (1985) 1042.
- [68] K. Edwards, J. Gustafsson, M. Almgren and G. Karlsson, *J. Colloid. Int. Sci.* 161 (1993) 299.
- [69] M. Ollivon, O. Eidelman, R. Blumenthal and A. Walter, *Biochem. J.* 27 (1988) 1695; see also, O. Eidelman, R. Blumenthal and A. Walter, *Biochem. J.* 27 (1988) 2839.
- [70] M.T. Paternostre, M. Roux and J.L. Rigaud, *Biochem. J.* 27 (1988) 2668.
- [71] P.K. Vinson, Y. Talmon and W. Walter, *Biophys. J.* 56 (1989) 669.
- [72] S. Almog, B.J. Litman, W. Wimley, J. Cohen, E. Wachtel, E.J. Barenholtz, A. Ben-Shaul and D. Lichtenberg, *Biochem. J.* 29 (1990) 4582.

- [73] D. Andelman, M.M. Kozlov and W. Helfrich, *Europhys. Lett.* 25 (1994) 231.
- [74] S. May and A. Ben-Shaul, *J. Chem. Phys.* (1995) in press.
- [75] D.P. Siegel, *Biophys. J.* 65 (1993) 2124.
- [76] M.M. Kozlov, S.L. Leikin, V. Chernomordik, V.S. Markin, and Y.A. Chizmadzhev, *Eur. Biophys. J.* 17 (1989) 121.
- [77] A.J. Verkleij, C.J.A. VanEchteld, W.J. Gerritsen, P.R. Cullis and B. DeKruiff, *Biochim. Biophys. Acta* 600 (1980) 620.
- [78] D.E. Leckband, C.A. Helm and J. Israelachvili, *Biochem.* 32 (1993) 1127.
- [79] R.P. Rand and V.A. Parsegian, *Biochim. Biophys. Acta* 988 (1989) 351.